Archs Sci. Genève	Vol. 56	Fasc. 1	pp. 11-38	Juillet 2003

PHOTOMETRY OF B-TYPE STARS IN THE GENEVA SYSTEM[1]

BY

Noel CRAMER[2]

ABSTRACT

Photometry of B-type stars in the Geneva system. - The Geneva seven-colour photometric system has been applied for more than four decades. Its data bank presently contains 373'000 measurements of 50'000 stars of all types. About 35% of the latter are of types O, B and first A, i.e. hotter than 10'000 K and more massive than 2.5 solar values. The light of these bright and massive stars is virtually without exception extinguished ("reddened") by interstellar dust, and its analysis has to account for that effect. Here, we illustrate the colorimetric properties of the system by means of some calibrations made in a 3-dimensional orthogonal reddening-free representation optimised for B-stars that separates temperature and gravity effects. Effective temperatures, bolometric corrections and absolute magnitudes are thus estimated. Central to all stellar photometric calibrations is the empirical determination of the intrinsic colours. A method for accurately determining the latter is described. The preliminary results of an application of the calibrations to the mapping of dark interstellar clouds within 2 kpc of the sun are presented. The unavoidable limitations imposed upon photometry by undetected causes of scatter, such as in binary systems, are mentioned. Open questions and future prospects are briefly referred to.

Key-words: B-type stars, Geneva photometric system, Calibrations, Fundamental parameters, Interstellar extinction.

1. INTRODUCTION

Astronomy is the only natural science where the objects of research, with the limited exception of those within our solar system, are physically inaccessible. All data pertaining to the universe at large down to our local stellar neighbourhood have to be gained by the passive analysis of incident electromagnetic and corpuscular radiation. Nevertheless, the amount of information conveyed by such radiation is vast and, as FRED HOYLE emphasised some 50 years ago in the prologue to his popular book Frontiers of Astronomy, "*The astronomer's problem is not a lack of information but an embarrassing excess of it. His is often a problem of disentanglement rather than one of synthesis*". Many techniques have been developed to that end. They resort as a whole to the physical analysis of starlight and of electromagnetic emission and absorption by interstellar matter at all wavelengths, as also to the precise measurement of stellar positions over the course of time by astrometry. The latter provides fundamental data that determine the cosmic distance scale and the tangential dynamical component of nearby stellar systems. The former enables us to spectrally analyse the *local* conditions of the emitting (or absorbing)

---

[1] Based on data acquired at the La Silla (ESO, Chile), Jungfraujoch and Gornergrat (HFSJG International Foundation, Switzerland), and Haute-Provence (OHP, France) observatories.

[2] Observatoire de Genève, CH-1290 Sauverny, Switzerland.
e-mail: noel.cramer@obs.unige.ch

media and to derive the prevalent physical quantities such as chemical composition, temperature, gas pressure as also their radial dynamical components. One of the fundamental observational quantities relevant to the electromagnetic spectrum is the photometric measurement of radiation in various well defined wavelength regions. Accurate "multicolour photometry" has thus been profitably applied since the nineteen fifties following the advent of sensitive photoelectric detectors, and is still one of the basic tools of observational astrophysics.

Of several multicolour systems in the visible (3000 Å to 6000 Å) which differ by the shapes and spectral domains of their passbands, the most important currently in use for ground-based observations are the "international" – or JOHNSON - UBV system, the STRÖMGREN uvby system and the Geneva system. Of these, the latter is the most homogeneous and in most applications also the most precise. Here, we will present a summary of the system's colorimetric properties followed by an overview of its applications to the analysis of the more massive ($M > 2.5\ M\odot$, $T_{eff} > 10000$ K) and luminous stars using methods specific to the Geneva system.

2. THE GENEVA SYSTEM

The Geneva seven-colour photometric system was defined in the late fifties by M. GOLAY and first used at the Sphinx Observatory of the Jungfraujoch Scientific Station in 1960. It has subsequently been applied at the Observatoire de Haute Provence (OHP), Gornergrat, Calar Alto (MPG) and the La Silla (ESO) Observatories and is currently in use at the IAC Observatory on the Island of La Palma of the Canary Islands. The passbands (fig. 1, RUFENER and NICOLET 1988; NICOLET 1996) were originally chosen with the intent of reproducing the general properties of the U,B,V system with the help of an identical V band but with slightly different U and B bands presenting less overlap at the BALMER jump of the hydrogen spectrum. The other four intermediate bands, B1, B2, V1 and G, were added in view of approximating the stellar classification properties of spectrophotometry involving the hydrogen absorption lines and gradients defined over the PASCHEN continuum as practiced in the nineteen fifties and early sixties at the Observatoire de Paris by CHALONGE and DIVAN using photographic techniques.

The initial reductions of the raw photometric measurements to their values outside our atmosphere and their normalisation by correlation to a standard system follow an elaborate series of processes and steadily increment the Geneva photometric data bank and its catalogue (see RUFENER, 1964). This will not be the subject of the present discussion which is based on the use of the standardised, catalogued data. In regard of the former, the Geneva system may be considered as "closed" (i.e. restricted duplication of instrumentation, single reduction procedure, limited observational sites; see RUFENER 1985) and the data are consequently extremely homogeneous and accurate. The important implication – exclusive to the Geneva system – is that calibrations, or any other procedures set up to extract information from the measurements, are unique. They can be applied equally well to all the available reduced data, even to those acquired several decades ago, without any particular adjustments being necessary. A general review of the

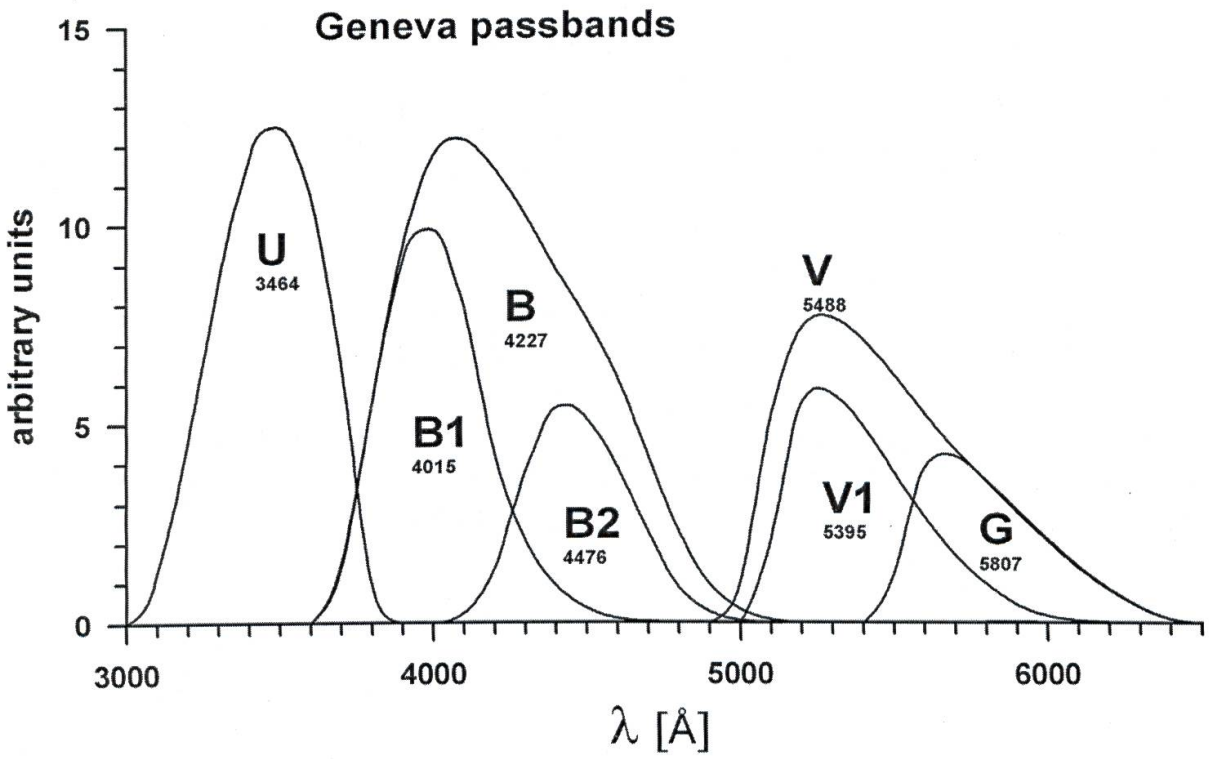

FIG. 1.

The passbands of the Geneva photometric system with an indication of their mean isophotonic wavelengths in angstroms .

system was presented earlier by GOLAY in Vistas in Astronomy (1980). The rapid sampling technique of measurement currently in practice, though by means of a photometer refurbished in 2001, is described by BURNET and RUFENER (1979) and BARTHOLDI *et al.* (1984). A concise historical summary of the Geneva system is given in CRAMER (1994, 1999) and references therein.

The data of the catalogue are presented conventionally in "magnitudes" which are logarithmic expressions of flux ratios:

If the radiation fluxes of two stars in a given spectral range are in the ratio f_1/f_2

$$m_1 - m_2 = -2.5 \log (f_1/f_2) \qquad \text{or, conversely} \qquad f_1/f_2 = 10^{-0.4(m_1 - m_2)}$$

The scale of the *apparent visual magnitudes* m_v (magnitudes in passband V) is adjusted relatively to a conventional zero point (where $m_2 = 0$) in this manner and which roughly corresponds to the brightest stars visible in the night sky. Increasing magnitudes imply decreasing flux.

Likewise, if the flux measurements of a *given* star are made in two wavelength ranges (passbands) C_1 and C_2, then the difference in magnitudes in these two ranges is the corresponding *colour index*:

$$C_1 - C_2 = m_{C1} - m_{C2}$$

To illustrate the general properties of colour indices we show the classical [U, B, V] (Geneva) diagram in fig. 2.

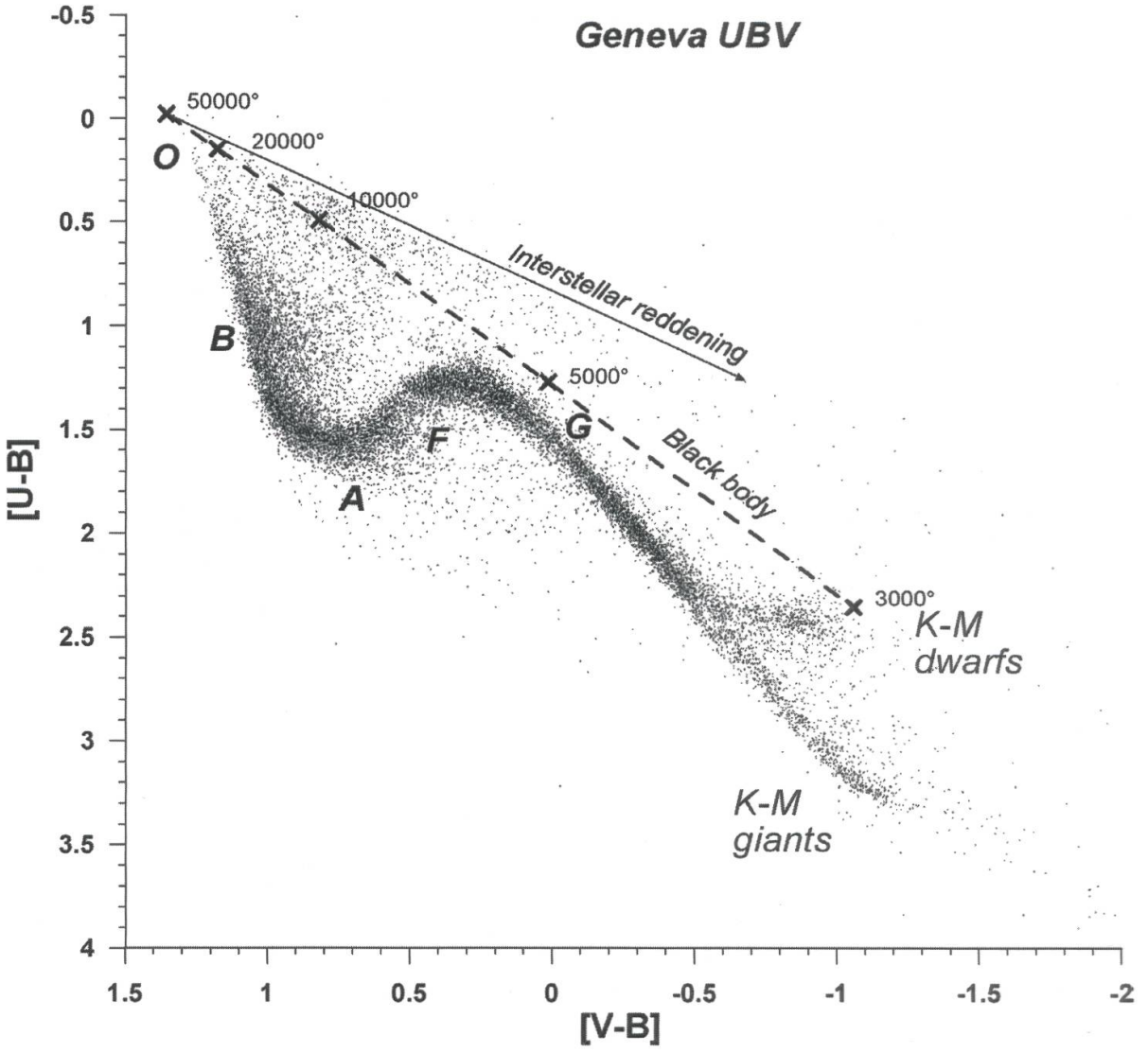

FIG. 2.

The UBV diagram in the Geneva system with location of the MK spectral types. Only $^1/_4$ of the measured stars are plotted for sake of clarity. The direction of the effect of interstellar extinction (reddening) by dust is indicated as well as the locus of black body radiation for various temperatures.

The sequence is basically a temperature sequence, as shown by the locus that would correspond to black body radiation of varying temperature in the same diagram. The departures from the black body are essentially due, at the higher temperatures, to the properties of hydrogen absorption in the stellar atmosphere (BALMER series and discontinuity due to the onset of continuous absorption) and at the lower temperatures to the apparition of molecular absorption. One also notes the large number of "reddened" O and B stars which appear to extend from the main sequence in the upper part of the diagram. Reddening is produced by wavelength-dependant absorption of starlight by interstellar dust. Passbands of shorter wavelength are most affected, and the corresponding colour indices involving other passbands are shifted red-ward by a "colour excess" that is proportional to the optical depth of dust traversed.

The dust grains responsible for interstellar reddening are very small – some 0.25 μm down to several angstroms. They are believed to consist largely of carbon in the form of graphite, and oxides of magnesium, iron and silicon. The direct evidence for graphite is the strong ultraviolet absorption feature at 2175 Å (see fig. 3) implying particles ≤ 0.015 μm, and for silicon oxides the presence of absorption bands in the infrared at 9.7 μm and 18 μm corresponding to amorphous silicates resembling olivine ($Mg_xFe_{2-x}SiO_4$). Another component related to carbon has recently been identified in the infrared with bands between 3.3 μm and 12 μm in emission. They are interpreted as being stretching modes of the C-C and C-H chemical bonds and imply the presence of polycyclic aromatic hydrocarbons (PAHs) on interstellar grains. Volatile compounds such as ices of water, methane, ammonia and other molecules composed of C, H, O, N can also be present in the cold conditions encountered in dark clouds, thus rendering the constitution of the dust particles sensitive to the intensity of the prevalent radiation field.

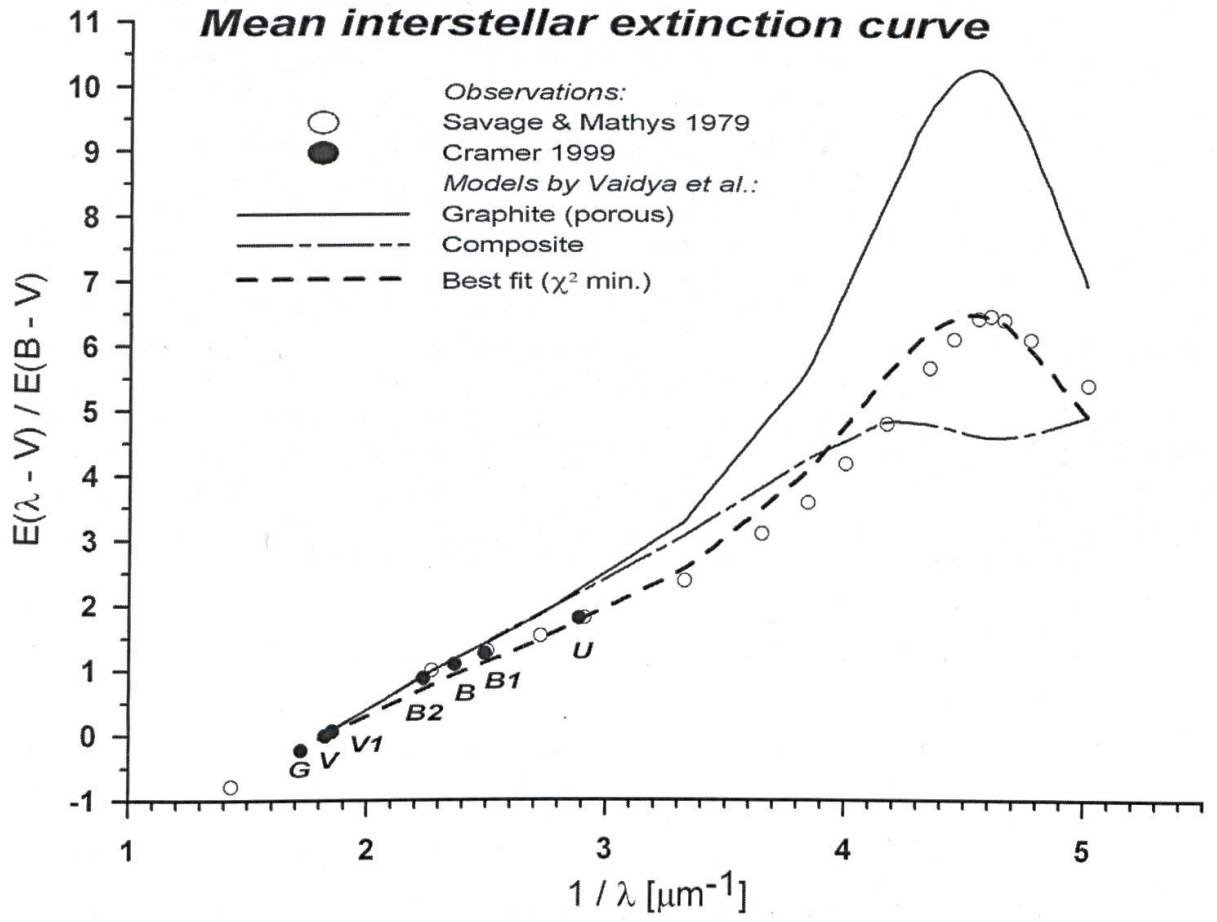

FIG. 3.

The mean interstellar extinction curve in terms of colour excess normalised to V (the vertical scale is sometimes given in terms of the absorption ratios A_λ/A_V). Observed values are by SAVAGE and MATHYS (1979), and by CRAMER (1999) for the spectral range covered by the Geneva system (see table 3, below). The models are one of a set computed by VAIDYA *et al.* (2001) for composites consisting of host silicate grains containing graphite inclusions and also associated with small "fluffy" porous graphite grains serving to reproduce the observed 2175 Å ($1/\lambda = 4.6\ \mu m^{-1}$) resonance of graphite absorption.

FIG. 3b.

Interstellar reddening illustrated by the dark cloud BARNARD 68. All the stars in the field are in the background and one sees their progressive "reddening" by dust extinction as the line of sight penetrates into the fringes of the cloud. Such dense "dark globules" are extreme examples of interstellar clouds consisting of gas and dust as they begin to contract and ultimately form new stars. BARNARD 68 is some 160 pc (500 light years) distant and only 0.2 pc in diameter. Observations in longer infrared wavelengths allow us to see through the central regions of the cloud and show that it is in the very earliest phase of collapse with no evidence of star formation yet (Three-colour composite obtained with VLT ANTU + FORS1, European Southern Observatory).

The interstellar medium is complex and diverse, and is not yet fully understood. The detailed composition of dust grains is still subject to much debate. But, in the near infrared and visible parts of the spectrum, extinction by dust is largely governed by MIE scattering (extinction coefficient $Q_\lambda \approx a/\lambda$ where a = grain size) as may be seen in fig. 3. Extinction by dust has been the subject of very extensive modelling and we show as an example in fig. 3 one (of several) computed by VAIDYA *et al.* (2001) that gives a good

account of the extinction curve in the visible. Models using different parameters reproduce the 2175 Å feature better, but are less satisfactory at longer wavelengths. We also show the portion of the curve rendered in terms of colour excess ratios derived empirically using 559 carefully selected O and B stars in the Geneva system (CRAMER 1999, or table 3, below). The overall agreement in the visible is very good.

Regarding the extinction seen in fig. 2, we may point out that highly reddened B stars, through their colour excesses in U-B and V-B, can become indistinguishable in certain cases from lower temperature stars by merging with the type A, F or G sequence in this 3-colour diagram. Therefore, further information (i.e. a better sampling of the spectrum by more passbands) is needed for the proper analysis of systematically reddened stars.

3. B-TYPE STARS IN THE GENEVA SYSTEM

3.1 Preliminary remarks

About 35% of the stars measured in the Geneva system can be loosely qualified in terms of the MK spectral classification as "B-type" (or, more precisely as O, B and first A-types). The hot, highly ionised, radiatively conducting atmospheres of these massive stars account for a relatively simple spectrum in the visible marked by the salient features of the BALMER jump and the hydrogen lines. Their spectral energy distribution, which is the dominant feature registered by multicolour photometry, is less affected by variations in chemical composition than that of their cooler counterparts. Moreover, such rapidly evolving and consequently young stars are not highly dispersed in initial chemical abundance (referred to as "metallicity" by astronomers) in our galactic neighbourhood since their population has not had time to be significantly subjected to mixing by galactic rotation. These factors reduce the colorimetric dispersion due to composition and contribute to simplify analysis in terms of basic quantities such as effective temperature and absolute magnitude.

B-type stars are, however, by their nature (short lifetime and lesser formation rate) much more sparsely distributed than cooler types, and their subsequently greater distances unavoidably link the study of their population by multicolour photometry to the effects of interstellar extinction by dust.

For effective temperatures higher than about 10^4 K, and in contrast to cooler stars, the vectors of interstellar reddening in colour index representations incorporating additional passbands such as B1, B2, V1 and G stand well separated from those related to variations of the other major astrophysical quantities. This allows us to de-redden such stars with confidence and, conversely, to study the distribution of interstellar dust efficiently by measuring the extinction via the resulting "colour excesses". It is therefore profitable, as in the present context, to go one step further by "projecting" colour index combinations along their reddening vectors, and thereby defining reddening-free "colour spaces" generated by new sets of colour parameters.

3.2 The reddening-free representation adapted to B-type stars

The Geneva photometric catalogue lists the average values of the *normalised* reduced colours U, V, B1, B2, V1, G and the V-magnitude m_v of each object. These colours are in reality the colour indices [U-B], [V-B], [B1-B], [B2-B], [V1-B] and [G-B] normalised to B. Square brackets are used by convention to distinguish the Geneva indices from those of other systems. The following relation converts the indices listed in the catalogue to magnitudes:

$$M_j = m_v - [V\text{-}B] + [j\text{-}B]$$

Where j is one of the 7 passbands.

The three traditional reddening-free parameters d, Δ and g of the Geneva system are each defined in the [U, B1, B2], [U, B2, G] and [B1, B2, G] diagrams, respectively (see for example GOLAY, 1980). A transformation in the three dimensional space generated by the above-mentioned parameters (CRAMER and MAEDER, 1979) leads to a new set of orthogonal parameters optimised for B-type stars and expressed here in terms of linear combinations of the normalised colours as follows:

$$X = 0.3797 + 1.3764\,U - 1.2162\,B1 - 0.8498\,B2 - 0.1554\,V1 + 0.8449\,G$$
$$Y = -0.8288 + 0.3235\,U - 2.3228\,B1 + 2.3363\,B2 + 0.7495\,V1 - 1.0865\,G$$
$$Z = -0.4572 + 0.0255\,U - 0.1740\,B1 + 0.4696\,B2 - 1.1205\,V1 + 0.7994\,G$$

- The X parameter has properties which are similar to those of the U-B index by measuring the BALMER jump via U-B1, but benefits of a larger range of variation and has the important advantage of being reddening-free. It is the optimal temperature indicator for B stars in the Geneva system.
- Y is much less sensitive to the BALMER discontinuity, but maximises the sensitivity to the width of the hydrogen lines via the B2-B1 index embedded in the relation. This makes it the best surface gravity indicator for B stars in the Geneva system (surface gravity determines the local gas pressure, which affects the collisional broadening component of absorption lines).
- Z is virtually independent of temperature and gravity effects. It optimises the detection of variations of gradient over the PASCHEN continuum in the range covered by the V band. Very weakly dispersed ($\sigma \cong 0.01$ mag) for normal B stars, it detects "peculiarity" (Ap, Bp stars) and has been shown to be correlated, in restricted cases, with the surface magnetic field intensity via the 5200Å absorption feature that characterises such stars (CRAMER and MAEDER 1980).

The typical probable errors over the indices and parameters are given in table 1, where the weight P is synonymous with the number of good measurements contributing to the mean value in the catalogue.

The general features of this 3-dimensional representation are shown in the two projections into the X,Y and Y,Z planes of figures 4 and 5 below.

Noteworthy is the rectilinear sequence in fig 4 along the X axis starting at type O down to the first A-types where effective temperatures sink to about 10^4 K. The second

TABLE 1.

Standard deviations of indices, visual magnitude and parameters (σ x10^3)

P	U	B	V	B1	B2	V1	G	mv	X	Y	Z
1	7.7	4.1	4.6	4.6	4.5	4.5	5.7	6.2	14.0	16.0	6.1
2	5.5	2.9	3.2	3.2	3.2	3.2	4.1	4.4	9.9	11.3	4.3
3	4.5	2.4	2.6	2.6	2.6	2.6	3.3	3.6	8.1	9.2	3.5
5	3.5	1.8	2.0	2.0	2.0	2.0	2.6	2.8	6.3	7.1	2.7
10	2.4	1.3	1.4	1.4	1.4	1.4	1.8	1.9	4.4	5.0	1.9

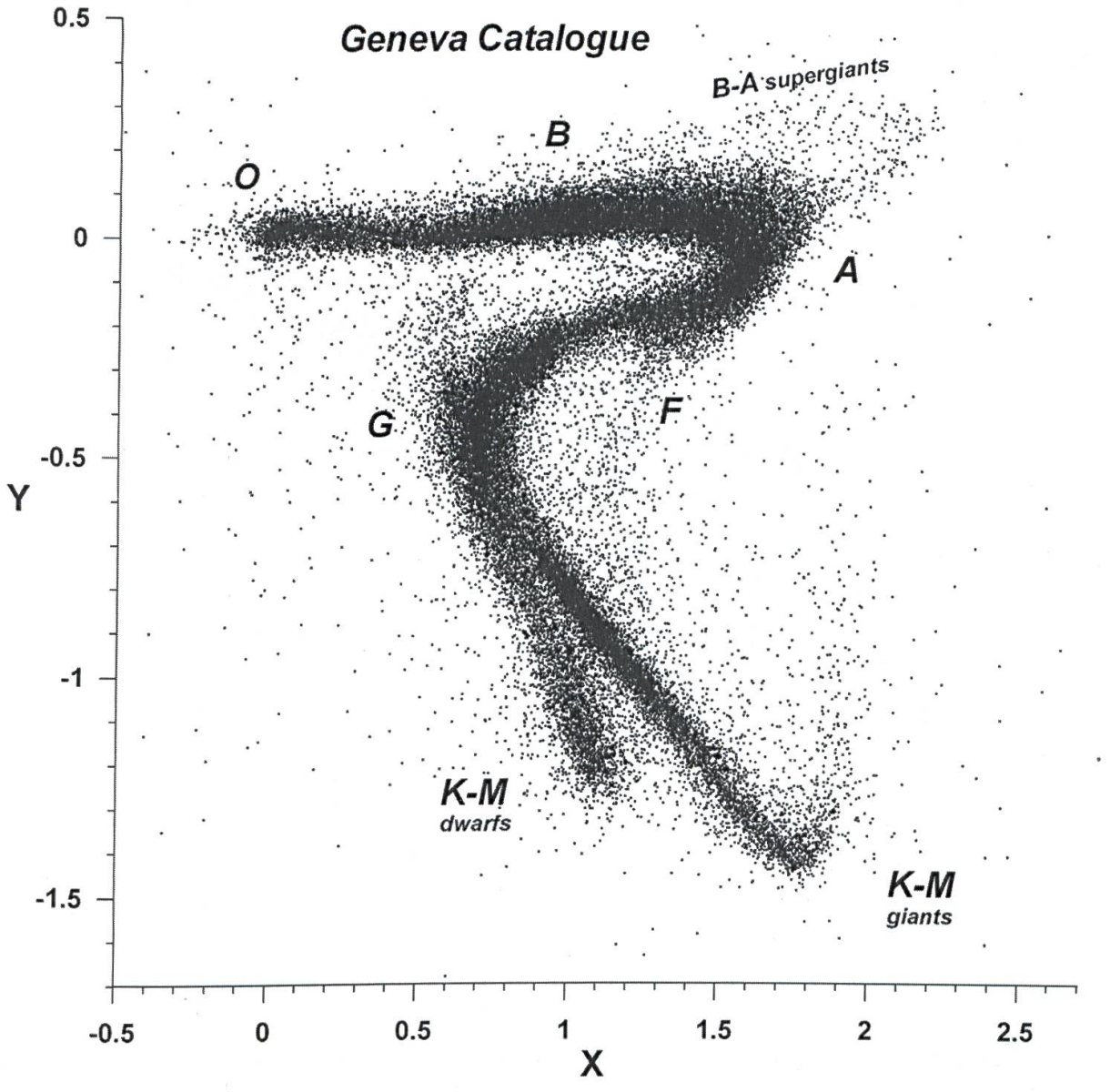

FIG. 4.

The reddening-free representation of the Geneva X, Y, Z parameters with an indication of the locations of the MK spectral types. The X, Y diagram shown here demonstrates the optimisation for the early-type stars (types O, B and first A) which occupy an almost rectilinear sequence along the X direction with a separation of the giants and supergiants from the non-evolved sequence.

important feature is the separation of evolved stars, culminating at the supergiant phase, from the non-evolved main sequence. The clean separation of the population of massive stars is put into better perspective by the Y, Z projection of fig 5, which also confirms that the X and Y parameters are the most relevant of the three in regard to the intrinsic physical properties of the former.

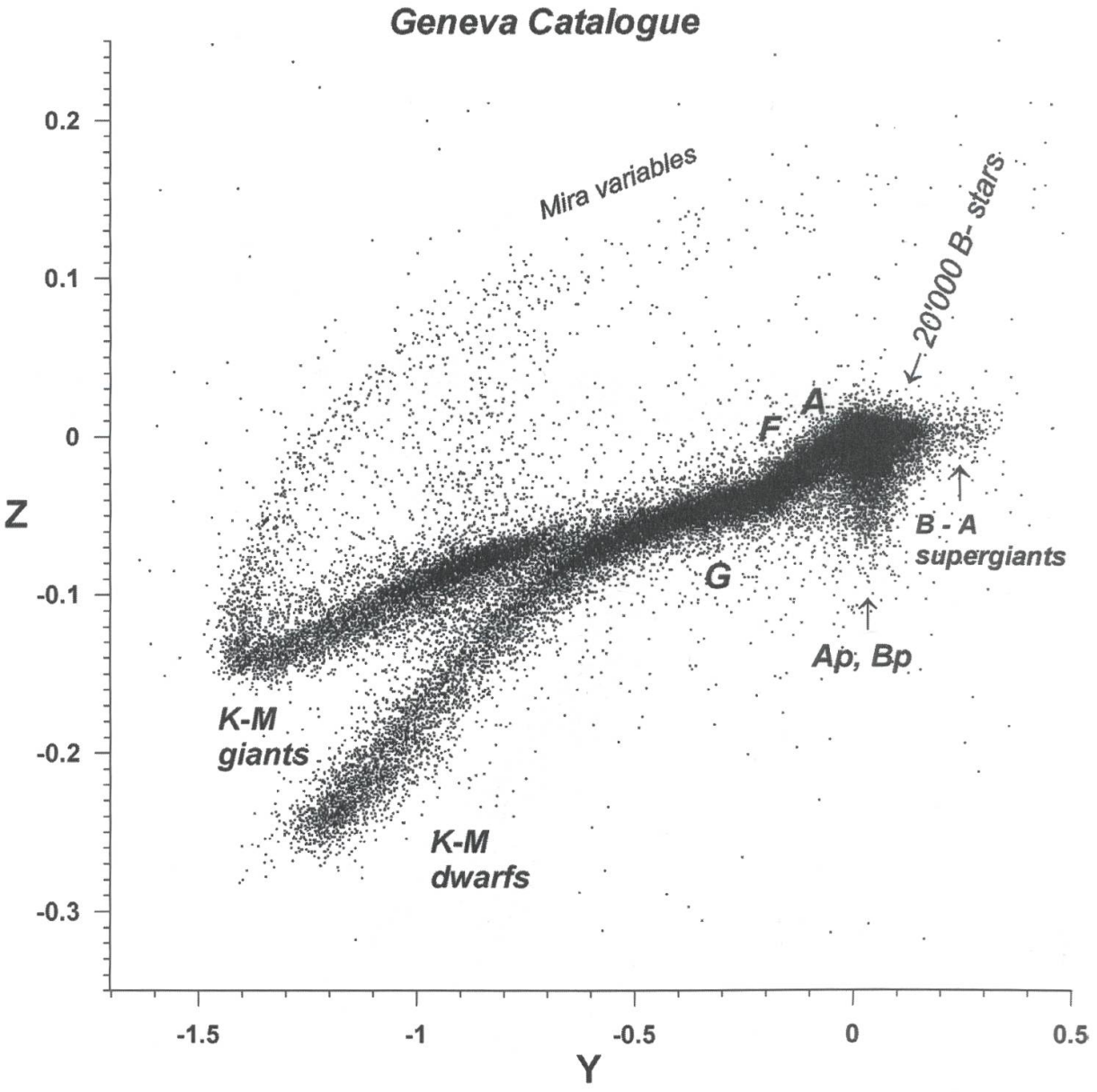

FIG. 5.

The Y,Z projection has the uncommon property of gathering about 20'000 O and B-type stars in the small clump to the right of the figure at Y=Z=0 thus demonstrating that two parameters (X and Y) suffice for their analysis. Those detaching themselves towards the extreme right are the early-type supergiants. Those descending and forming a sort of "beak" are the magnetic Ap and Bp stars.

3.3 Calibrations

A simple confinement of the region occupied by the B-type stars in terms of the three X,Y,Z parameters ($Y > -0.08$ and $0.05 > Z > -0.01$) isolates that population and

enables a set of calibrations to be made with little ambiguity regarding the estimate of basic stellar physical properties such as:

- The effective temperature T_{eff}. If F is the electromagnetic flux (erg s^{-1} cm^{-2}) emitted by the star at *its surface*, the "effective temperature" T_{eff} is defined by convention in terms of the STEFAN-BOLTZMANN radiation law by $F = \sigma(T_{eff})^4$
- Surface gravity $g = GM/R^2$ expressed in cm s^{-2}. Most often, its logarithmic expression is used.
- Absolute magnitude in the V passband M_v. The absolute magnitude M_v is by convention the apparent magnitude in the V band, m_v, of the star seen at a distance of 10 parsecs (1 parsec = 3.2616 light-years = 3.0857 10^{18} cm) in absence of interstellar extinction.
- Bolometric correction BC. The correction to M_v necessary to obtain the total absolute (bolometric) magnitude integrated over the whole spectrum, $M_{bol} = M_v + BC$. This value is important for evaluating stellar luminosity L (total radiation energy output per unit time), a basic parameter in theoretical stellar modelling. L is generally referred to the solar value $L\odot = 3.85\ 10^{26}$ W. Knowing that $M_{bol}\odot = 4.74$ mag, we have: $M_{bol} = 4.74 - 2.5 \log(L/L\odot)$, thus defining L. More generally, we have $L = 4\pi R^2\sigma(T_{eff})^4$, which links the above mentioned quantities.
- Intrinsic colours. The true colour indices in the absence of interstellar extinction, thus also enabling the quantitative estimate of the interstellar extinction in each colour by comparison with the observed values.

The corresponding calibrations will be presented in the same order.

Photometric calibrations are essentially achieved by correlating in an optimum manner the observable photometric quantities with particular physical quantities that have been determined otherwise. The search of that "optimum" is the most important initial step of the process. Quite generally, the strategy of the analysis will depend on the properties of the system – i.e. the way its different passbands sample the energy distribution – and on the quantity to be estimated. Optimisation includes the search for simplicity, which is ideally also that of the minimal set of assumptions – or parsimony - regarding the calibration data. Thus, one gives greatest weight to "primary" physical data, whereas data of the same nature but derived via a more elaborate series of processes is given less weight, if not discarded altogether. Even primary data do, however, "evolve" with time as instrumental techniques get better – e.g. trigonometric parallaxes determined by spacecraft or the application of large interferometric telescope complexes to determine fundamental parameters such as stellar angular diameters – and some types of calibrations will therefore stay more "robust" than others depending on their dependence on such data.

The advent of good theoretical stellar atmosphere models has decisively contributed to the interpretation of multicolour photometry during these two last decades. Synthetic photometry done by filtering theoretical fluxes through sets of passbands links the basic physical quantities (temperature, surface gravity, chemical composition) inherent to the

models with the observed fluxes and helps to determine the regions where colour-colour diagrams perform best, thus also revealing the best shape of a possible calibration relation. Such a method will not, however, provide a workable calibration by itself because synthetic photometry is heavily hampered by "assumptions" affecting the models as well as the true shapes of the passbands. An example of such a synthetic "calibration" of the X, Y parameters in terms of effective temperature and surface gravity for the most massive stars by means of solar composition models computed by KURUCZ (1993) is given in fig 6. Even if the zero points and scales are not perfectly accurate, the general shape of such a relation is presumably true, and empirical – i.e. "minimally assuming" – fundamental data can be profitably used to adjust it in most cases (see for example KÜNZLI *et al.* 1997). The models also point out the existence of regions of ambiguity such as for the temperatures lower than 10'000 K at Y $\approx$ -0.2 in fig 6, where calibrations are impracticable in this parameter space.

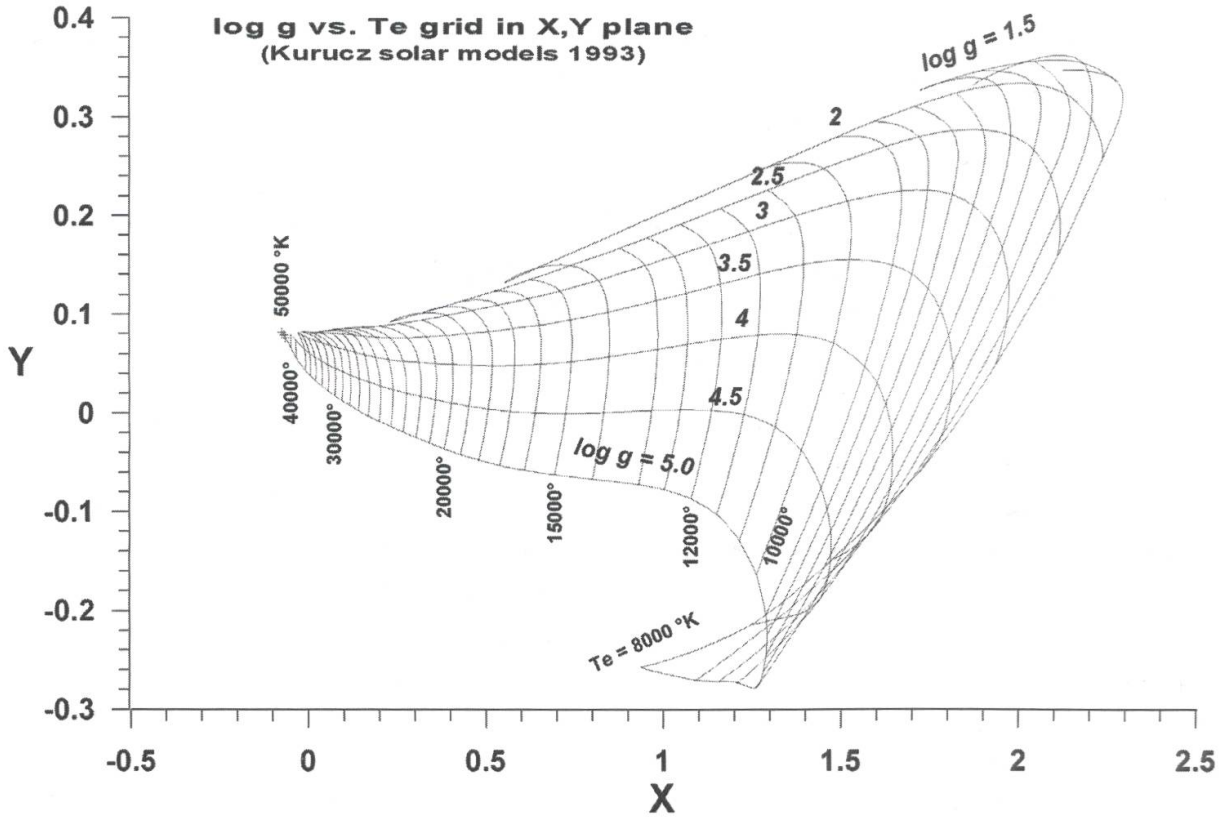

FIG. 6.
Synthetic grid of the stellar atmosphere models computed by KURUCZ (1993) in the X, Y diagram. Such theoretical projections of physical parameters into representations that are observationally determined offer precious guidelines to their interpretation.

Gravity and temperature are also the physical quantities that characterize the MK spectral classification. Their good separation in the restricted X, Y plane of fig 6 enables straightforward correlations to be made. The corresponding MK calibration of the X, Y parameters is described and tabulated in CRAMER (1999).

3.4. Effective temperatures and bolometric correction

As seen in fig 2, effective temperature is one of the "first order" effects of multicolour photometry due to its colorimetric nature. The literature is well bestowed in calibrations, either photometric or spectroscopic, and their resulting estimates of T_{eff}. Fundamental empirical data of that sort are, however, still not very common for the most massive stars due to technical reasons, and one has to go back to the original interferometric work of CODE *et al.* (1976) for the most direct estimate of T_{eff} of a few nearby stars obtained with the 188 m baseline Narrabri intensity interferometer in Australia. Empirical calibrations of effective temperatures and bolometric corrections based on the results of CODE *et al.* and using the X parameter alone have been presented elsewhere

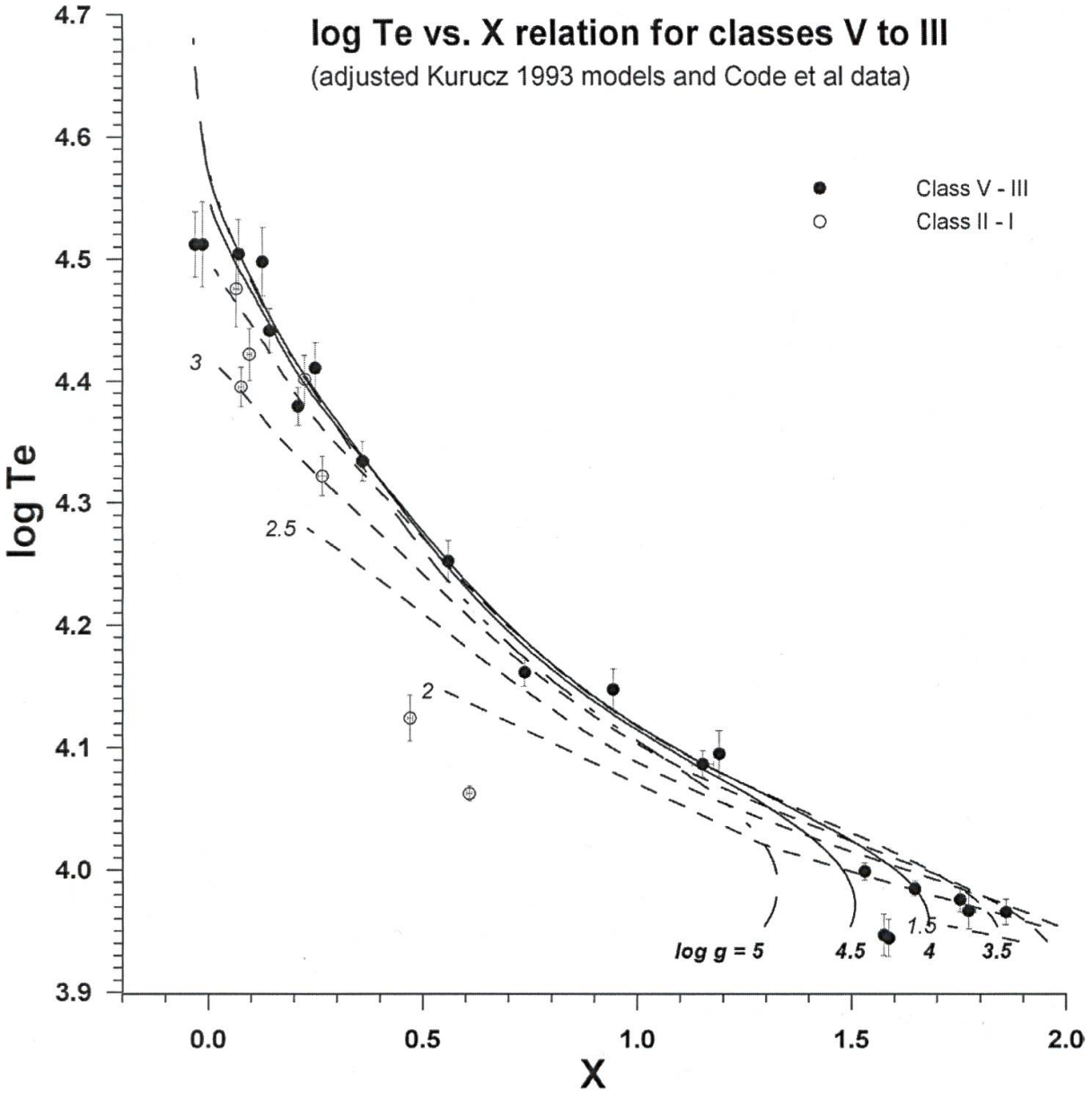

FIG. 7.

KURUCZ's (1993) models adjusted to fit a log T_{eff} versus X relation through the empirical data of CODE *et al.* for O, B and first A stars of classes V to III. The lines of lower gravity as well as the values of the bright giants and supergiants have been included for purposes of comparison only.

(CRAMER and MAEDER 1979; CRAMER 1984). Here, we go a step further by using the shape of the T_{eff} versus X relation predicted by synthetic photometry to fit the data. The result presumably takes better account of the "physics" that underlie the form of the sequence and is shown in fig. 7.

The empirical data displayed correspond to the class V to III O-B stars of CODE *et al*'s (1976) list, where the stars that the authors corrected for duplicity have also been adjusted here to reproduce the colours of the primary. A small shift (0.035 mag) of the X values of the (KURUCZ 1993) solar models was made to optimise the fit (see discussion and tabulation of the calibration in CRAMER, 1999).

The bolometric correction computed by KURUCZ is adjusted in the same manner, and the corresponding bolometric corrections of the models are given in fig. 8.

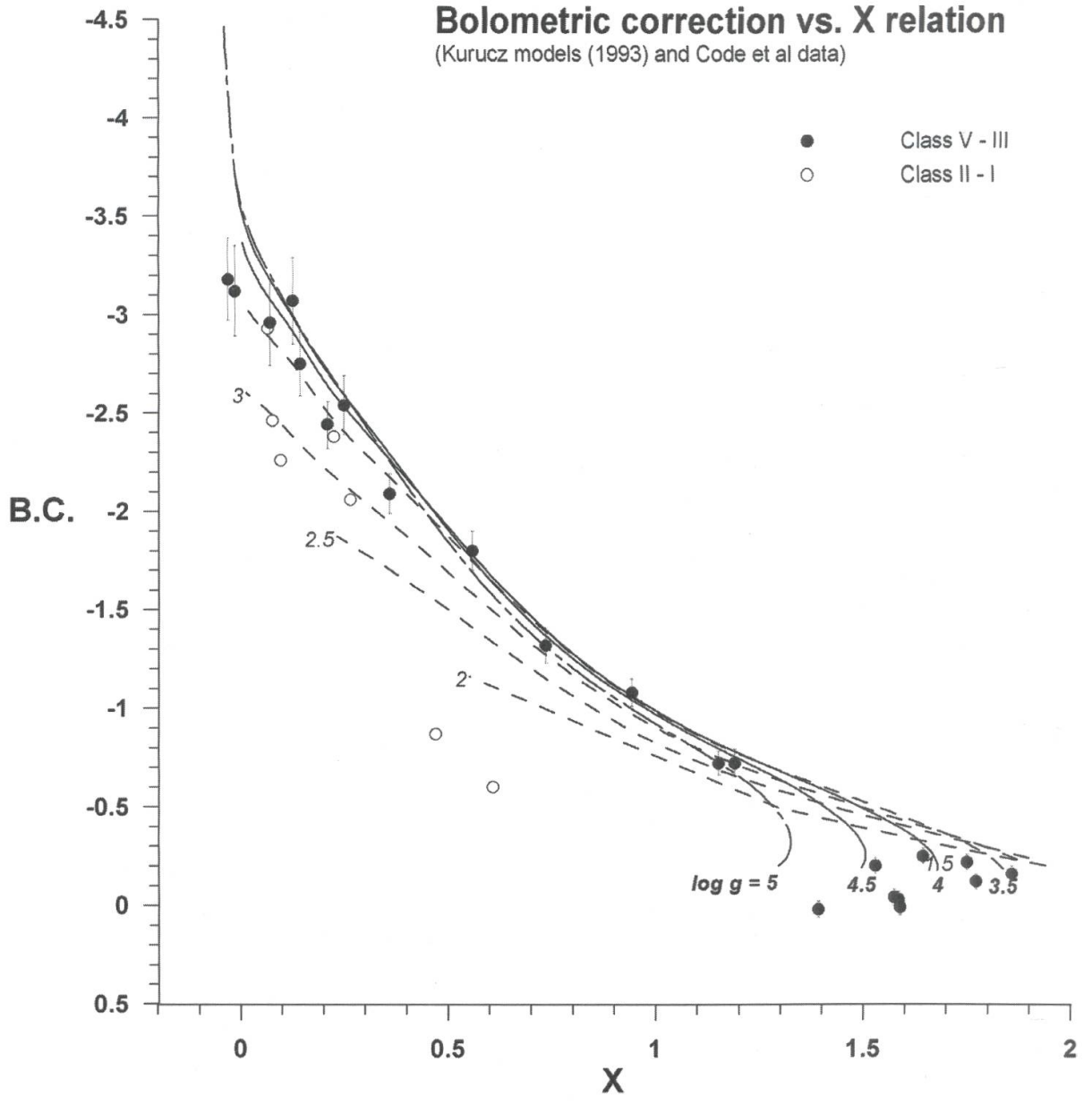

FIG. 8.

Synthetic relations for the bolometric correction compared with those of CODE *et al*. Same comments regarding adjustment as for fig. 7.

They also agree perfectly with those of CODE *et al.* A detailed tabulated form of these two calibrations can be found in CRAMER (1999) as well as comments regarding a determination of surface gravity, log g, with the aid of the Y parameter. However, satisfactory estimates of these quantities that agree well with the empirical data can also be expressed for stars within the log g = 3.5 to 4.5 range by the following third degree polynomials:

$$\text{Log Te} = 4.5424 - 0.7138\,X + 0.3785\,X^2 - 0.0894\,X^3 \qquad \text{for log Te} \geq 4$$

And

$$\text{B.C.} = -3.3501 + 3.6156\,X - 1.4928\,X^2 + 0.2551\,X^3 \qquad \text{for B.C.} \leq -0.02$$

The straightforward relation between X and effective temperature for the main sequence and slightly evolved (log g $\approx$ 3.5) B-type stars as seen in these relations calls for a comparison with effective temperatures determined by a different method in the same spectral range. A comprehensive list of T_{eff} established by SOKOLOV (1995) shares 225 bright stars in common with our data within the validity range of our calibration. SOKOLOV's effective temperatures are derived via a measurement of the BALMER jump and the gradients of the adjacent BALMER and PASCHEN continua using spectrophotometry in the near ultraviolet and the visible in a manner akin to the classical photographic method of CHALONGE and DIVAN. The method critically depends on a number of assumptions requiring a well established calibration of the relationship between those gradients and the BALMER jump versus T_{eff} (and gravity), well measured and homogeneous continuum energy distributions as well as a good correction of interstellar reddening. The comparison of the data is shown in fig. 9.

Even though the reported probable errors are relatively large, a systematic overestimate of T_{eff} is apparent in the B2 to B7 spectral range for SOKOLOV's T_{eff}. Incidentally, such an overestimate is noted by SOKOLOV himself regarding T_{eff} estimates by MOROSSI and MALAGNINI (1985), and appears to hold also in our simpler and "less assuming" context. It is difficult to accept the discrepancy in fig. 9 in view of the substantial agreement between the photometric parameters, KURUCZ's models and the fundamental data of CODE *et al.* in the present context. This comparison serves to illustrate the above-mentioned necessity to rely as far as possible on primary data, within a context of parsimony, while establishing a new calibration.

3.5. Absolute magnitudes

The determination of absolute magnitudes is a fundamental issue of astronomy and astrophysics. The basic distance scale is determined astrometrically through trigonometric parallaxes and in some cases that were formerly beyond the reach of the latter, by the nearby moving cluster method (Sco-Cen, Hyades). Photometric and spectroscopic calibrations by means of cluster colour-magnitude sequences have been subsequently scaled to that fundamental, but restricted, sample of nearby stars. The recent results of the Hipparcos astrometric satellite (released in 1997) have significantly improved our knowledge regarding the trigonometric distance scale. One of the initial motivations for the definition of the X, Y, and Z parameter space was to establish an absolute magnitude

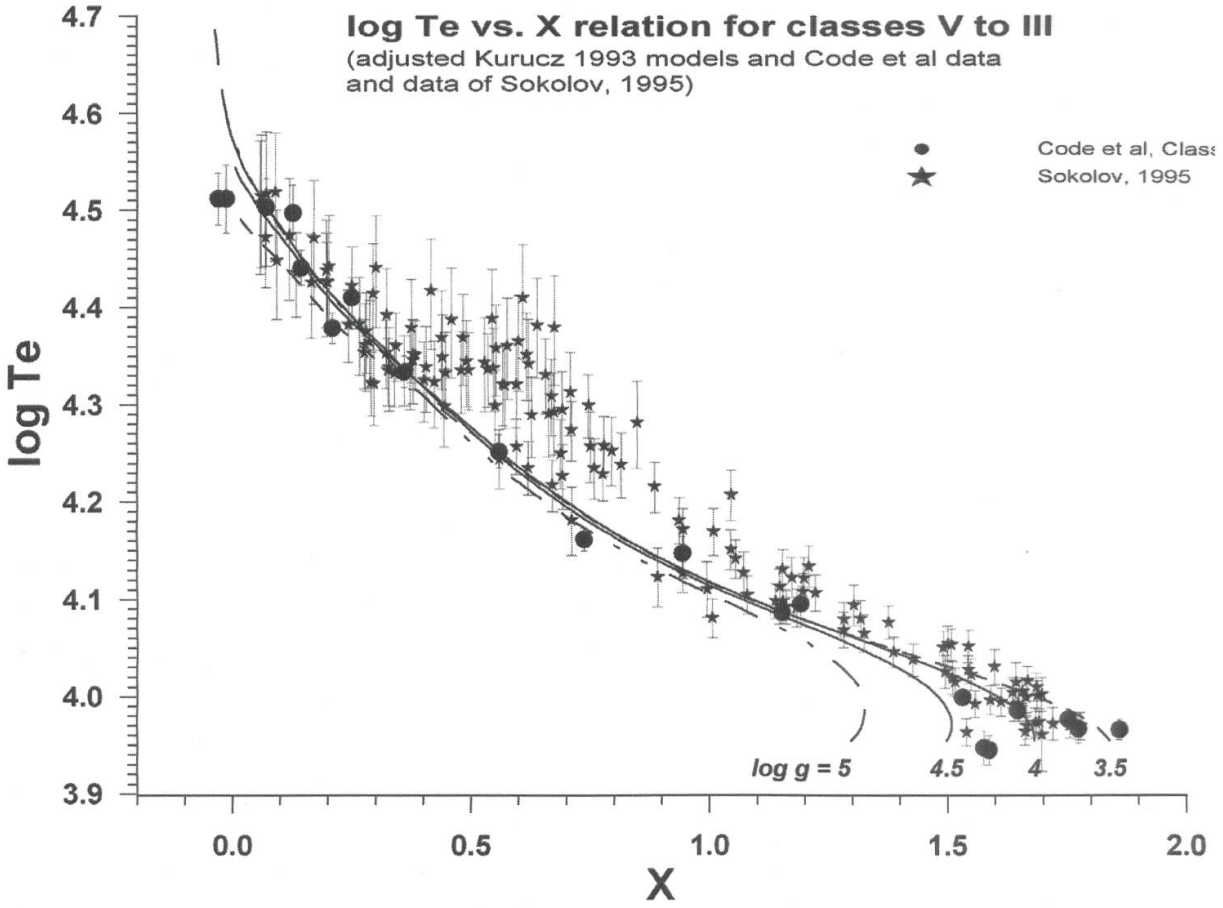

FIG. 9.

KURUCZ's (1993) models adjusted as in fig 7 compared with T_{eff} derived by SOKOLOV (1995) for 225 bright early type stars common to the Geneva catalogue. In spite of the probable errors, SOKOLOV's estimates are systematically larger in the B2 - B7 spectral range.

calibration which would allow field stars to be integrated into studies of stellar evolution (CRAMER and MAEDER 1979). Virtually no primary measurements of distance (apart from the nearby Scorpio-Centaurus association) were available for B stars at that time, and the calibration relied essentially on cluster distance modulus determinations published in the literature. The reference data were voluntarily biased against multiplicity (two, or more closely located stars observed as "one" star), when possible, (some 50% of early-type stars are members of binary- or multiple systems) and included a few bright giants and supergiants. The global standard deviation over the residuals amounted to 0.38 mag for the first calibration sample of 199 stars used in 1979.

Subsequently, several calibrations were made with the object of improving the estimate and expanding (if possible) the range of validity. There too, the biasing toward single stars was carried out by an iterative process. The brightness of binaries (or multiples) is systematically underestimated in an absolute magnitude versus colour relation, shifting those belonging to clusters artificially into the foreground. Such stars were removed from the basic sample until the distributions around the mean estimated cluster distances became symmetrical. For those calibrations also, the standard deviation over the residuals was found to be no better than 0.40 mag.

The most objective and precise distance data were finally provided for early-type stars in the solar neighbourhood by the Hipparcos satellite late in 1996. This enabled a totally independent calibration to be undertaken on the basis of 6044 field B- to A stars and 134 members of the Scorpio-Centaurus association. After selection over well defined parallaxes, their locations in the X, Y diagram ($Y \geq -0.06$) and discrimination against known binaries (including those detected by Hipparcos), 1580 stars of classes V to III remained for the calibration. These were then de-reddened and provided the reference sample of M_V. The resulting calibration surface is shown in fig 10 where it is also mapped into the X, Y plane with the calibration stars.

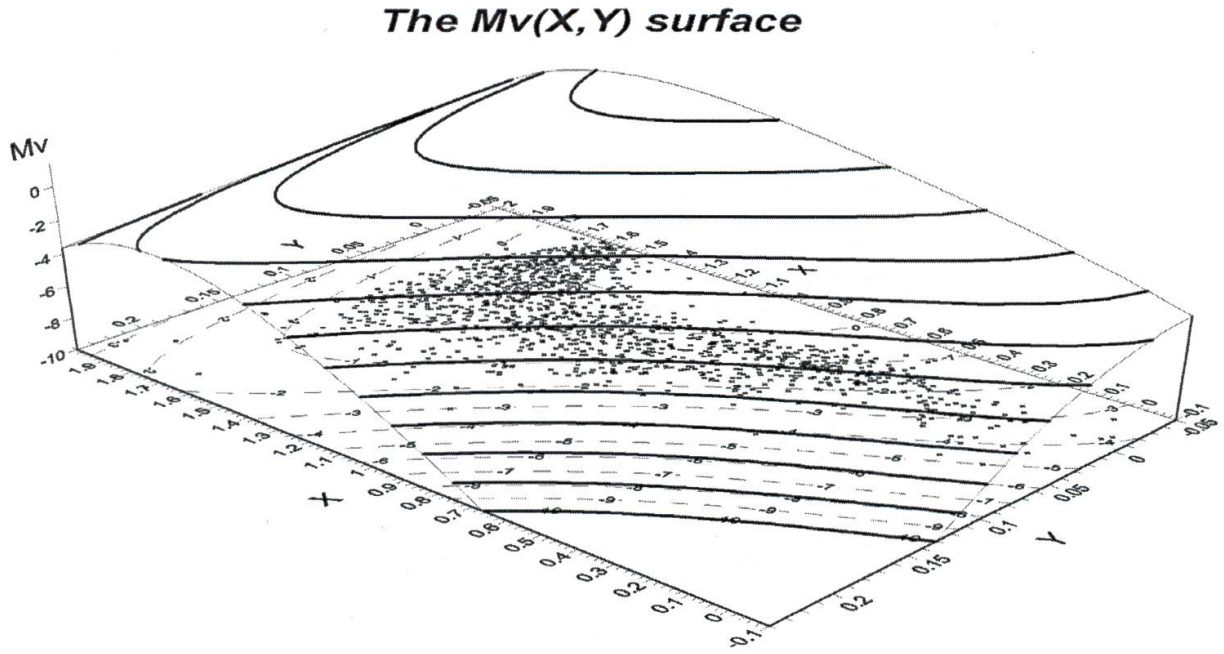

FIG. 10.

Absolute magnitude calibration of the X,Y diagram based on the Hipparcos satellite parallaxes. The calibration stars are plotted in the projected figure.

The following polynomial form, of fourth degree in X and quadratic in Y, defines the new $M_V(X, Y)$ relation:

$$M_V(X, Y) = a_0 + a_1Y + a_2Y^2 + a_3X + a_4XY + a_5XY^2 + a_6X^2 + a_7X^2Y + a_8X^2Y^2 + a_9X^3 + a_{10}X^3Y + a_{11}X^4$$

With

a_0	a_1	a_2	a_3	a_4	a_5	a_6	a_7	a_8	a_9	a_{10}	a_{11}
-3.7528	-21.0189	-161.4130	5.2076	-2.5839	138.1530	-2.8463	13.2480	-29.8913	2.9365	-4.0510	-1.2997

Here too, the standard deviation over the residuals (after subtraction of the statistical component of uncertainty inherent to Hipparcos) amounts to 0.44 mag, and is comparable to those of the earlier calibrations. A sizeable part of these ubiquitous four tenths of a magnitude of uncertainty arises from the gradient of the calibration acting on the uncertainties of measurement over the parameters themselves. The mean internal standard deviation surface of $M_V(X,Y)$ estimated with the help of the total differential of

the calibration relation is given with its mapping into the X,Y plane, in fig. 11, including the 12'800 well measured stars in the colour domain of fig. 10. It clearly shows that an uncertainty of the order of 0.20 mag is unavoidable for purely metrological reasons.

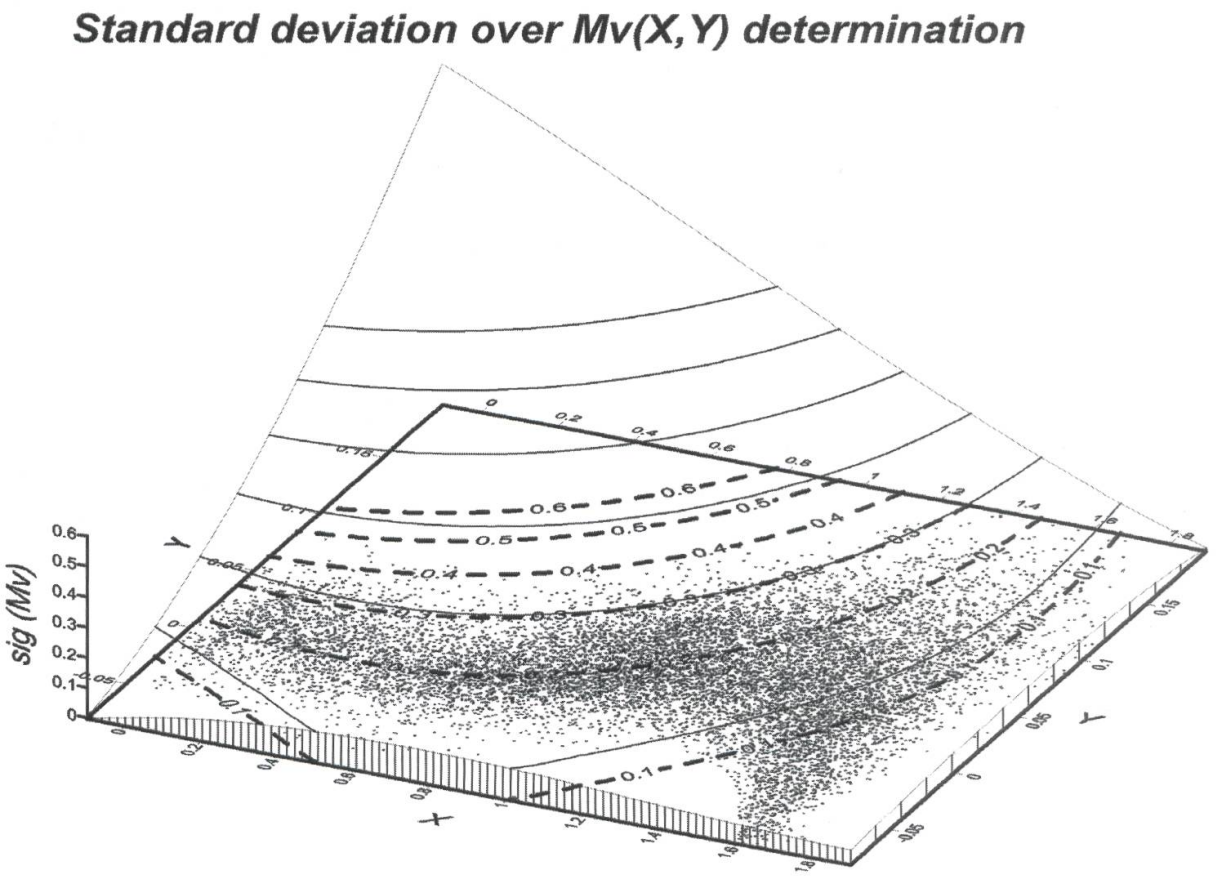

FIG. 11.

The internal standard deviation surface of the $M_V(X,Y)$ absolute magnitude calibration and its projection onto the X,Y plane. The stars of the Geneva catalogue in the same colour domain of fig 10 are plotted in the figure. An error ranging from 0.1 mag to about 0.4 mag, depending on the local declivity of the relation, can be expected for metrological reasons alone. Intrinsic uncertainties of that order are common to all photometric estimates of M_V, of individual stars in the upper main sequence.

Among the underlying astrophysical causes of dispersion, stellar rotation can be expected to contribute typically by about 0.1 mag (see CRAMER and MAEDER 1979). However, binarity still remains the major perturbing agent of an M_V calibration. An example of the importance and complexity of the binarity "loops" for this calibration is illustrated in fig 12 within a restricted region of main sequence stars corresponding to types B6.5 to B8.5 with indication of the δM_V of the components. The effects of binarity in a photometric diagram depend on the shape of the related sequence and quite generally lead to an underestimate of the true luminosity of the pair. For stars of types later than B8V ($X \geq 1.1$), the variation of colour due to a bend in the lower sequence generates an error on the estimate that may even exceed the 0.753 mag that would be caused by an identical twin.

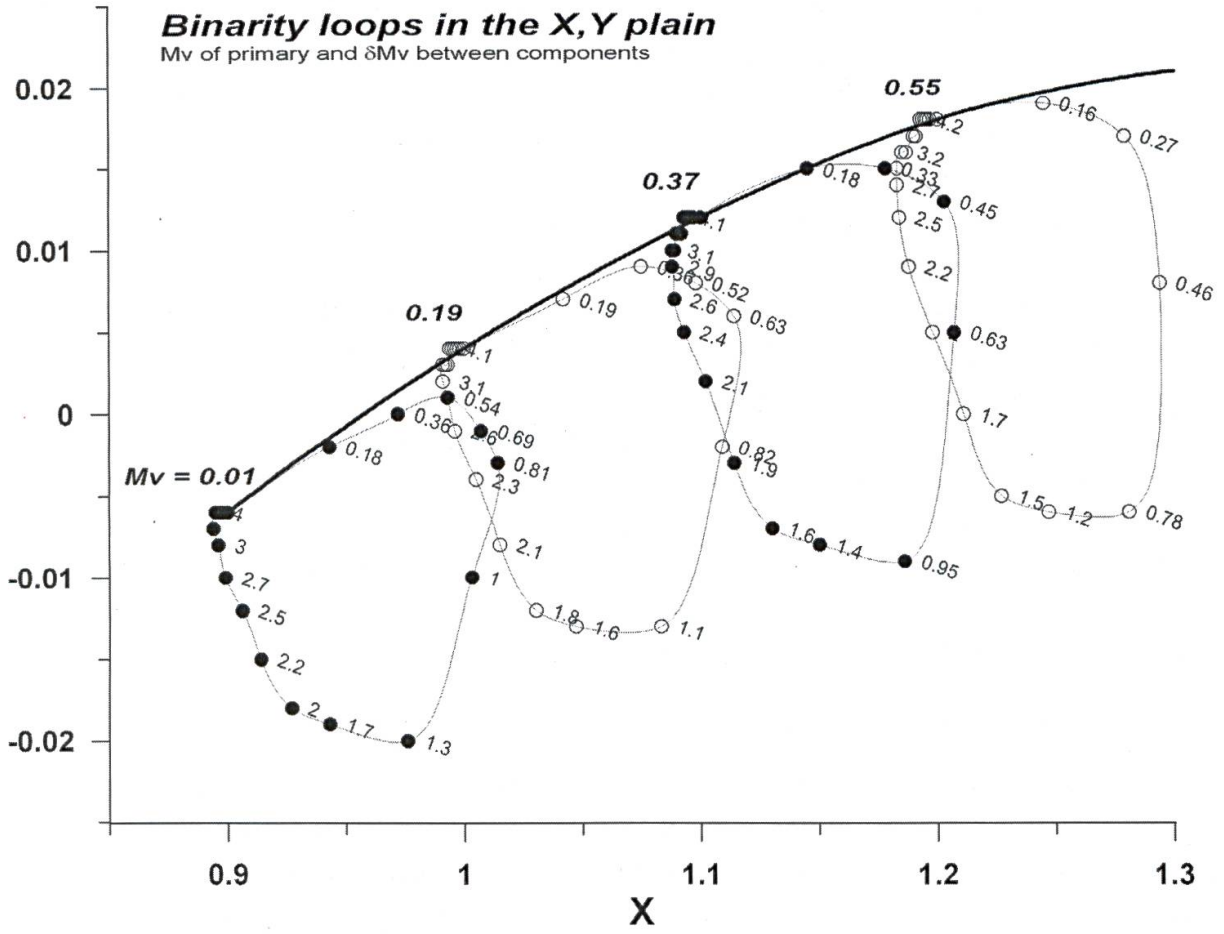

FIG. 12.

Effects of binarity in the X, Y diagram. The loops are computed here by adding a string of less luminous stars from a ZAMS (Zero Age Main Sequence) to a variety of primaries of class V. The zone is restricted here to stars corresponding to classes B6.5 to B8.5 in view of better illustrating the influence of the difference in magnitudes dM between the two components.

Various estimates of the frequency of binaries among B stars encountered in the literature lie within the range of 40% to 50%, i.e. more than half of the whole population of individual stars of that type are members of a system. If a secondary is detected and the relative contributions of the components can be estimated, standard calibrations can be applied after the corresponding corrections have been made to the observed colours. Otherwise, and actually in a large proportion of cases, the results derived by photometric calibrations will be affected by unseen companion stars. The establishment of a calibration itself may therefore be motivated by two different points of view.

The first is to assume that it is impossible to assemble a perfectly "clean" sample of single reference stars large enough to carry out a "pure" calibration. In any case, when applied randomly and on a large scale to the real population of stars, such a calibration would systematically be biased. So, for statistical investigations, a calibration based on a consistently non-selective sample of data would be most suitable.

The second approach is to strive to establish a calibration that is as pure as possible. The major difficulty then lies in the choice of the data, some of which will have to be corrected for multiplicity. Part of which will nevertheless also be contaminated by still undetected binaries. Empirical calibrations voluntarily biased in favour of single stars will have to be used carefully in statistical studies. They are, however, best suited for comparisons with synthetic predictions or for the interpretation of theoretical models which generally concern single stars.

In fact, neither of these two objectives is fully attained. For the advocates of the first, the temptation to repress evidently peculiar data during the calibration process is difficult to resist. For the second, the sheer volume of potentially valuable but marginally suspect data that have to be discarded causes a painful dilemma for the "calibrator". So, whatever may be the character of a given calibration, multiplicity remains a major source of noise, and the accurate assessment of its incidences is difficult. Hence, the persistent dispersion of the residuals in the various attempts to calibrate M_V, as mentioned above, should not be considered as a cause of concern but rather as the sign of an inevitable limitation of the photometric method.

3.6. The intrinsic colours problem

The knowledge of the intrinsic colours of a stellar population in a given photometric system is of fundamental importance. It is a necessary condition for all calibrations of physical parameters in the system. De-reddening of stellar groups or of individual stars can only be properly carried out if the corresponding intrinsic colours are known. Comparisons of synthetic photometry based on stellar models with observations must be done relatively to an accurate, but empirically consistent sequence. In the particular case of the inevitably distant O and B stars, reddening is always intimately connected with the observations. It is not possible to define a non-reddened sequence in colour-colour or colour-magnitude diagrams by simply using the observed "blue envelope", as may be more legitimately done in some cases for cooler nearby stars, provided their chemical compositions are not too dispersed. The blue envelope will unavoidably be affected by some residual reddening and will also favour peculiar objects. A pertinent process of extrapolation applied to normal stars of the population has to be utilised for the calibration. It will be all the more accurate the closer one is able to approach the conditions of "minimal assumption" regarding the processing of the calibration data.

Synthetic photometry of stellar atmosphere models can at first glance be seen as a possible aid in the process. It is, however, heavily burdened with assumptions as mentioned earlier. It may nevertheless be, as for effective temperatures, of precious assistance through its prediction of the expected shape of the relation or, even better, by its a posteriori confirmation in that regard of a completely empirical calibration. The latter case has proved to be essentially true for the empirically derived intrinsic colours of O and B stars of classes V to III in the Geneva system (see detailed discussions in CRAMER 1982, 1993, 1999), which then served to rectify the synthetic photometry. The results are presented below in table 2 in the form of empirically derived intrinsic colour estimators:

TABLE 2.

Coefficients of the intrinsic colour estimators $[k\text{-}B]_0(X,Y)$

$$[k\text{-}B]_0(X,Y) = a_0 + a_1X + a_2Y + a_3XY + a_4X^2 + a_5Y^2 + a_6XY^2 + a_7X^2Y + a_8X^3 + a_9Y^3$$

Where k = U, V, B1, B2, V1, G

Index	a_0	a_1	a_2	a_3	a_4	a_5	a_6	a_7	a_8	a_9
[U-B]	0.0380	0.9057	-0.0625	-0.2409	-0.0518	4.8627	-2.6551	-0.0340	0.0240	1.9123
[V-B]	1.3431	-0.3227	0.2400	-0.3371	0.1582	1.6294	-1.1422	0.4078	-0.0638	-5.4104
[B1-B]	0.7413	0.0937	-0.2001	-0.0480	-0.0152	1.0014	-0.5845	-0.0249	0.0067	1.6738
[B2-B]	1.6408	-0.0878	0.2403	0.0721	0.0061	-2.3129	1.2373	-0.0151	-0.0039	1.6564
[V1-B]	2.0062	-0.2480	0.0974	0.4180	0.0752	-6.2176	3.1873	-0.0139	-0.0350	0.8075
[G-B]	2.5758	-0.2907	0.0734	0.4734	0.0823	-9.9578	5.3204	0.0013	-0.0398	1.1033

These estimators define the zero points regarding interstellar extinction of the colour indices (i.e. the intrinsic colours) of any star of class V to III within the parameter range discussed above. The corresponding "colour excesses" are then for each colour Cl, respectively, $E_{[Cl]} = Cl_{(observed)} - Cl_{(intrinsic)}$ and serve to estimate the quantity of extinction by interstellar dust in the given colour.

The significant advantage of these estimators over similar methods utilised in other photometric systems is their ability to estimate intrinsic indices of individual stars *regardless of prior knowledge of their evolutionary stage* (within the class V to III limits) in virtue of the sensitivity of the Y parameter to gravity. This is of great value for studies of field stars, but can also be used to good effect in the cases of associations or clusters masked by unevenly distributed foreground reddening (see RABOUD *et al.* 1997) or even in studies involving distinct star clusters merged by chance along the same line of sight (see CARRIER *et al.* 1999).

The overall accuracy of the $E_{[B-V]}$ estimate is reckoned to be better than 0.02 mag. The *internal* statistical error depends on the accuracy of the measured [B-V] index, on that of the X, Y parameters and on the local slope of the calibration relation as in the case of the Mv(X, Y) estimator (fig. 11). In the present case, its value varies between 0.004 and 0.010 mag.

Further basic quantities in the interpretation of colour index diagrams of reddened stellar populations are the ratios between the respective colour excesses. The prior knowledge of the intrinsic values reduces the process to a set of straightforward correlations established over samples of stars with different extinction. We have chosen here to correlate all the two-by-two combinations of Geneva colours with the [B-V] colour excess, since that index is universally used to express interstellar reddening, and the results are given in table 3. Incidentally, these ratios also describe the interstellar extinction curve in the visible (fig. 3, above).

Other ratios, not involving the [B-V] index, can easily be derived from these values. The visual absorption A_v is also readily estimated for all indices with the help of these relations (The absorption in magnitudes in the V passband is: $A_v = 2.75\ E_{[B-V]}$, in the mean, for B stars in the Geneva system).

TABLE 3.
Colour excess ratios relative to [B-V]

CI	E [CI]/E [B-V]	σ	CI	E [CI]/E [B-V]	σ
U-B	0.654	0.003	B2-G	1.014	0.003
B1-B	0.158	0.002	U-V1	1.597	0.004
B2-B	-0.195	0.002	U-G	1.861	0.005
V1-B	-0.943	0.002	U-V	1.654	0.003
G-B	-1.208	0.003	B1-V1	1.100	0.003
U-B1	0.497	0.001	B1-G	1.364	0.004
B1-B2	0.351	0.001	B1-V	1.157	0.002
B2-V1	0.750	0.002	V1-V	0.062	0.002
V1-G	0.266	0.003	G-V	-0.210	0.003
U-B2	0.848	0.003	B2-V	0.807	0.002

The calibrations of intrinsic colours and colour excess ratios presented here for the O, B and earliest A stars of classes V to III are specific to the observational data of the Geneva system. They have been derived through a totally empirical process and with minimal recourse to external data. They are arguably the most robust that can be achieved within their limited range. The zero-points rely most heavily on the observed colours of the closest stars. These had all been well measured at the time the calibration was first established (CRAMER, 1982) and the accumulation of new data does not have any significant incidence regarding an improvement of their accuracy. Their exclusively empirical nature renders them ideally suitable for comparisons with more elaborately derived quantities such as those proposed by synthetic photometry, as mentioned earlier.

The large scale behaviour of reddening determined in this manner is partially illustrated in fig 13 with the $E_{[B-V]}$ versus distance diagram for regions centred on the galactic plane within ±3 degrees of latitude, whereby the distances are derived by the $M_v(X, Y)$ calibration (note that $m_{v0} = m_v - 2.75\ E_{[B-V]}$ for B stars in the Geneva system and that $E_{(B-V)Johnson} = 0.842\ E_{[B-V]Geneva}$). The plot shows, as expected, rather strong absorption by interstellar dust. The minimum extinction gradient related to the most transparent lines of sight is seen to be close to $2\ 10^{-4}$ mag/pc, roughly corresponding to space densities of $3\ 10^{-14}$ dust grains cm^{-3} (i.e. about one 0.2 μm grain per 320 m cube). The solar system is situated in a very empty region of space where the density of neutral hydrogen is $n_H \leq 0.1\ cm^{-3}$ (one cm^3 of gas at sea-level pressure would have to be expanded into a column 50 pc long!).The first strongly dust-absorbed regions appear at about 500 pc, in the vicinity of the OB associations in Cygnus.

The two corresponding higher and lower galactic latitude plots in both hemispheres (not shown here) are not very different in their overall properties, except for presenting directions of even greater transparency at high latitudes, as expected. The southern hemisphere sample is better populated due to the greater number of measurements obtained there. They both show the first significant onset of extinction at about 150 pc, corresponding to the nearby young star-forming regions in the GOULD Belt that is inclined by approximately 18° relatively to the galactic plane.

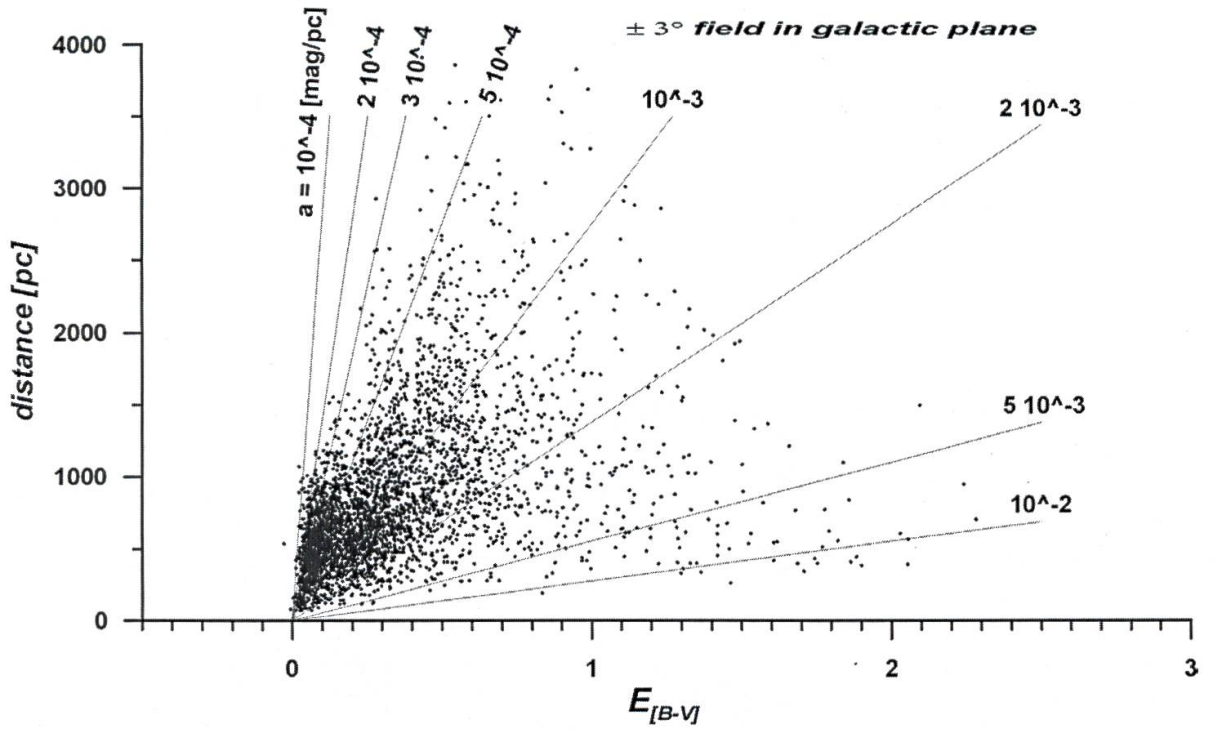

FIG. 13.

Estimated colour excess versus distance within a 6° wide strip centred on the galactic equator for 3600 stars in the validity range of the calibrations. Several reddening lines corresponding to different values of constant extinction are plotted. A gradient of 2 10^{-4} mag/pc gives a good account of extinction in the most transparent regions within the first kiloparsec and roughly corresponds to a particle density of 3 10^{-14} grains cm^{-3}. The distances are derived here with the $M_V(X,Y)$ relation calibrated with Hipparcos satellite parallaxes.

The availability of some 8000 estimates of distance and colour excess carried out in this manner enables a much finer three-dimensional investigation of the nearby interstellar dust clouds to be made. An analysis using an inverse method akin to current tomography techniques has very recently been carried out by VERGELY *et al.* by means of the mentioned data. The method is highly computation–intensive but has the advantage of largely eliminating the formation of radial heliocentric biasing that inevitably occurs with an indiscriminate use of error prone distance estimates. Though yet unpublished, we mention some of the salient features revealed by that study in the galactic plane.

As expected, dust clouds are detected in relation with the GOULD belt. Notably the Ophiuchus complex in the direction of the galactic centre and above the plane at some 150 pc, or the Orion complex, below the galactic plane, at $l \approx 210°$ with $d \approx 500$ pc. Otherwise, if we limit our view strictly to the galactic plane as in fig. 14:

- Between $l = 45°$ and 60° no dust clouds are seen up to 1 kpc, but at $l = 60°$ to 90° a dust complex at about 500 pc forms a "bridge" between the Saggitarius galactic arm and the Orion-Cygnus arm (on the inner border of which our Sun is located).
- Between $l = 100°$ to 140°, a large dust cloud is encountered at 300 pc.

- Between l = 210° and 270°, space is largely transparent until a patchily distributed and extensive arc of dark clouds is met at about 1.2 kpc. An isolated cloud is found at 1 kpc in the direction 270°.
- Another inter-arm "bridge" is suggested at about 1.5 kpc between l = 260° and 290°.
- At l ≈ 290° in the Eta Carinae direction, a number of absorbing structures are detected between 100 pc and 1.5 kpc.

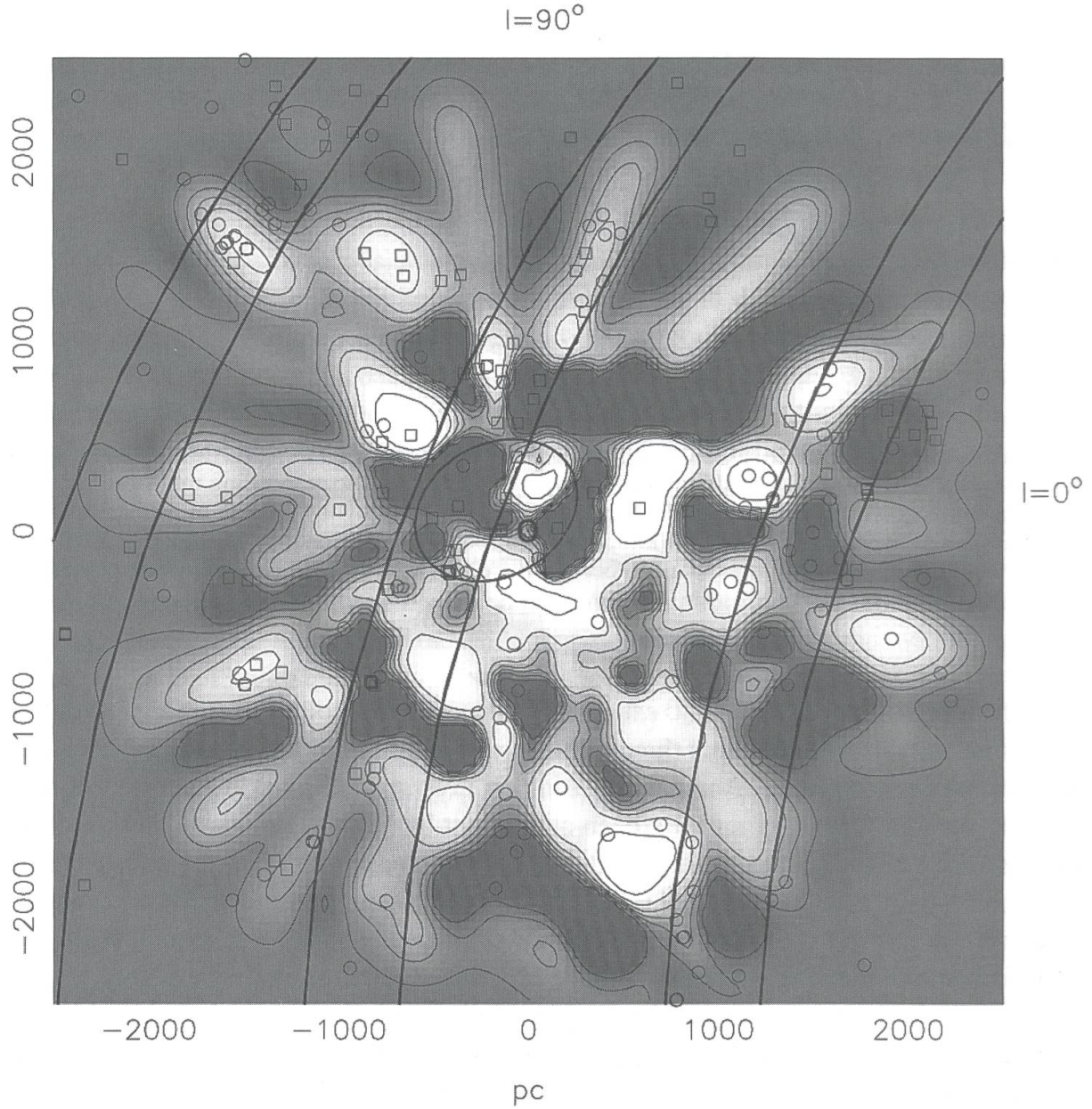

FIG. 14.

Distribution of opacity of the interstellar medium in the galactic plane and in the solar neighbourhood. The figure is a cross-section of the 3-dimensional opacity distribution derived by VERGELY et al. Centred on the Sun, it also shows the position of the GOULD belt (ellipse at centre) as well as (from left to right) the bands corresponding to the Perseus, Orion-Cygnus and Sagittarius arms. Open squares are H II regions, open circles are young open clusters. The galactic centre lies in the direction l = 0, to the right. The apparition of radial features beyond 2 kpc is due to the scarcity of our data at those distances.

FIG 14b.

The spiral galaxy M 74 (NGC 628). At a distance of 10.7 Mpc (35 million light years) and slightly smaller in size and stellar population than our own galaxy (about 30 kpc in diameter), M 74 is oriented face-on and gives a good idea of what we would see if we were able to travel a few hundred kpc above our galactic plane. The spiral structure is highlighted by vast amounts of gas and dust that provide the basic materials for star formation. Young star forming regions rich in hot massive stars give the bluish tinge to the less central parts of the spiral arms. The redder central regions of the galaxy are more densely populated by older, less massive and cooler stars as well as occasional evolved red giants. Our galaxy would, however, present more tightly woven spiral arms and portray a larger and slightly elongated ("barred") central bulge. The yellow circle has been scaled so as to put into context the heliocentric region of 2 kpc radius explored in fig 14 relatively to our position in our own galaxy, and illustrates its very local nature. Such a "small" sampling would not be suited to infer the large scale spiral structure of our galaxy (Radio- and infrared wavelengths are applied to that purpose). Our study does, however, show that dust lanes are not uniquely distributed along the spiral arms but also tend to bridge them, as seen at several locations in M 74. (Photo: Gemini North Observatory, GMOS team, Hawaii).

Though several dust structures are associated with spiral arms, no evident overall correlation seems to exist between extinction by dust and spiral arm indicators such as H II regions and young clusters. In our galactic neighbourhood, dust structures are distributed in the inter-arm regions and tend to "bridge" the arms.

The detailed discussion of the method used, including 3-D cartography with density distribution of the mentioned features and a comparison with the literature is done in the work by VERGELY *et al.*

4. Concluding remarks

The present discussion has emphasised the colorimetric properties of the Geneva system regarding the B-type stars, i.e. the system's ability to classify those stars and estimate basic physical parameters that are directly related to their spectral energy distribution. A discussion of the analysis of cooler (T_{eff} < 9000 K) stars for which multicolour photometry is much more strongly influenced by variations of chemical composition has not been attempted. Different strategies have to be followed for optimising calibrations in that domain (see GRENON, 1978, 1981, MENNESSIER and GRENON, 1985, or GRENON 1993, for that matter). Neither has the application of Geneva photometry to the study of stellar variability, and its astrophysical implications, been mentioned (see for example BURKI, 1999 or CARRIER *et al.* 1999). Nor have we talked about the record, of unquestionable geophysical interest, that spans more than 40 years and consists of the measurements of atmospheric transparency which are a by-product of the photometric reduction technique (see RUFENER, 1986 and BURKI *et al.* 1995).

The object of this work has been to inform the reader regarding the general properties of the Geneva photometric system and, within the restricted context of the most massive stars, show how basic physical parameters may be derived in spite of extinction by interstellar dust. And that, indeed, the suppression of that "troublesome effect" leads to an estimate of its distribution in interstellar space.

The essential elements of a "toolbox" have been provided in the form of calibrations (see CRAMER, 1999 for a more thorough treatment).

Looking toward the future, we may mention that the Geneva system has very recently been replicated using 2-dimensional CCD detectors. Good calibration and standardisation (a difficult task if the high accuracy of the current system is to be equalled or even surpassed) will extend the capability of sampling stellar populations beyond the present range of about 2 kiloparsecs. Data acquisition will be greatly increased. Regarding B stars, the result will be that departures from the locally prevalent reddening law will become more pronounced and, in particular, significantly different values of metallicity will be encountered among the stellar populations. New strategies will have to be developed to detect and estimate those variations and the calibrations will have to be adapted accordingly.

Ultimately, a much higher rate of data acquisition (ground-based or from space) with very high accuracy regarding flux measurement and passband definition would tend to justify the quest for a better optimised system that, within a relatively short period of a few years (or months), could replace the current photometry and render it obsolete. But

the present data bank with its homogeneous and highly accurate data spanning more than forty years would still remain a most valuable and unique record.

RÉSUMÉ

PHOTOMÉTRIE DES ÉTOILES DE TYPE B DANS LE SYSTÈME DE GENÈVE

Le système photométrique en sept couleurs de Genève est appliqué depuis plus de quatre décennies. Sa banque de données comprend actuellement quelque 373'000 mesures individuelles de 50'000 étoiles de tous les types spectraux. Environ 35% de ces dernières sont des types O, B et A précoces, c-à-d de température effective plus élevée que 10'000 K et de masse supérieure à 2.5 valeurs solaires. La lumière de ces étoiles brillantes et massives est pratiquement sans exception atténuée ("rougie") par la poussière interstellaire, et son analyse doit s'affranchir au préalable de cet effet. Ici, nous illustrons les propriétés colorimétriques du système au moyen de quelques calibrations établies dans une représentation tridimensionnelle, orthogonale et insensible au rougissement interstellaire. Les températures effectives, corrections bolométriques et magnitudes absolues sont ainsi estimées. La détermination des couleurs intrinsèques est intimement liée à l'application des calibrations photométriques. Une méthode pour déterminer ces couleurs avec précision est décrite. Les résultats préliminaires d'une cartographie des nuages obscurs interstellaires dans une périphérie de 2 kpc obtenue au moyen de ces calibrations sont présentés. Les limitations inéluctables qu'imposent des facteurs de dispersion non détectés, tels que la multiplicité, sont mentionnées. Des questions ouvertes et des développements futurs sont signalés.

Mots-clés: Etoiles de type B, Système photométrique de Genève, Calibrations, Paramètres fondamentaux, Extinction interstellaire.

REFERENCES

BARTHOLDI, P., M. BURNET, F. RUFENER, 1984, Three statistical tests for digital photometry, A&A 134, 290.

BURKI, G., F. RUFENER, M. BURNET, C. RICHARD, A. BLECHA, P. BRATSCHI, 1995, The atmospheric extinction at the E.S.O. La Silla observatory, A&AS 112, 383.

BURKI, G. 1999. Geneva photometry of the Be star HR 1960: periodicity and extremely small amplitude, A&A, 346, 134.

BURNET, M., F. RUFENER, 1979. A computerized differential photometer for the Geneva Seven Colour Photometric System, A&A 74,54.

Carrier, F., G. BURKI, C. RICHARD, 1999. Geneva photometry of the open cluster NGC 2451 and its exceptional Be star HR 2968, A&A, 341, 469.

CODE, A. D., J. DAVIS, R. C. BLESS, R. HANBURY BROWN, 1976. Empirical effective temperatures and bolometric corrections for early-type stars, ApJ. 203, 417.

CRAMER, N., A. MAEDER, 1979, Luminosity and T_{eff} determinations for B-type stars, A&A 78,305.

CRAMER, N., A. MAEDER, 1980. Relation between Surface Magnetic Field intensities and Geneva Photometry, A&A 88, 135.

CRAMER, N. 1982. Geneva [U,B,V] Intrinsic Colours of B-type Stars, A&A 112, 330.

CRAMER, N. 1984. Relations between U, B, V intrinsic colours and Geneva photometry for B-type stars. The effective temperature scales, A&A 132, 283.

CRAMER, N. 1993. Intrinsic colours of O, B and early A-type stars in the Geneva system, A&A 269, 457.

CRAMER, N. 1994. Geneva Photometry and its Homogeneity, review article in The impact of long term monitoring on variable star research, NATO ASI, (C. Sterken, M. De Groot, eds.), Kluver Acad. Publ., Dordrecht, 405.

CRAMER, N. 1999. Calibrations for B-type stars in the Geneva photometric system, review article, New AR 43, 343.

GOLAY, M. 1980. The Geneva Seven Colour photometric system, review article in Vistas in Astronomy 24, part 2, A. Beer, K. Pounds, P. Beer eds., Pergamon Press, Oxford.

GRENON, M. 1978. Propriétés photométriques des étoiles,G,K,M en relation avec la structure et l'évolution galactique (Thèse), Publ. Ob. Genève, Série B, Fascicule 5.

GRENON, M. 1981. Abundances, temperatures and reddening of field and cluster population II giants, In Astrophysical Parameters for Globular Clusters, IAU Coll. 68.

GRENON, M. 1993. Low-level stellar variability, In Inside the Stars, IAU Coll. 137, ASP Conf. Ser., Vol. 40, W.W. Weiss and A. Baglin (eds.).

KÜNZLI, M., P. NORTH, R. L. KURUCZ, B. NICOLET, 1997. A calibration of Geneva photometry for B to G stars in terms of T_{eff}, log g and [M/H], A&AS 122, 51.

KURUCZ, R. L. 1993. KURUCZ CD-ROM 13, ATLAS9 stellar atmosphere program and 2 km/s grid.

MENNESSIER, M. O., M. GRENON, 1985. A reddening and metallicity-free temperature estimator for late M giants, in Calibration of fundamental Stellar quantities, IAU Coll. 111, (D.S. HAYES *et al.*, Eds.) Reidel Publ. Co., Dordrecht.

MOROSSI, C., M. L. MALAGNINI, 1985. Observed and computed spectral flux distribution of non-supergiant O9 – G8 stars : III Determination of T_{eff} for the stars in the Breger Catalogue, A&AS 60, 365.

NICOLET, B. 1996. Geneva photometric passbands from the natural system, Baltic Astronomy 5, 417.

RABOUD, D., N. CRAMER, P. A. BERNASCONI, 1997. Geneva photometry in the young open cluster NGC 6231, A&A 325, 167.

RUFENER, F. 1964. Technique et réduction des mesures dans un nouveau système photométrique stellaire (Thèse), Publ. Obs. Genève A, 66, 413.

RUFENER, F. 1985. Approaches to photometric calibrations, in Calibration of fundamental Stellar quantities, IAU Symp. 111, (D.S. Hayes *et al.*, Eds.) Reidel Publ. Co., Dordrecht, 253.

RUFENER, F: 1986. The evolution of atmospheric extinction at La Silla, A&A 165, 275.

RUFENER, F., B. NICOLET, 1988. A new determination of the Geneva photometric passbands and their absolute calibration, A&A 206, 357.

SAVAGE, B. D., J. S. MATHYS, 1979. Observed properties of interstellar dust, review article, Ann. Rev. A&A, 17, 73.

SOKOLOV, N. A. 1995. The determination of T_{eff} of B, A and F main sequence stars from the continuum between 3200 Å and 3600 Å, A&AS 110, 553.

VAIDYA, D. B., R. GUPTA, J. S. DOBBIE, P. CHYLEK, 2001. Interstellar extinction by composite grains, A&A 375, 584.

VERGELY, J.-L., N. CRAMER, B. VALETTE, G. BURKI. Large scale dust structures in our Galaxy, A&A, (in press).